Statistical Properties of the DGD in a Long-Haul Optical Fiber System With Temporally Drifting Birefringence

Hai Xu, *Member, IEEE*, Brian S. Marks, *Member, IEEE*, John Zweck, Li Yan, *Member, IEEE*, Curtis R. Menyuk, *Fellow, IEEE*, and Gary M. Carter, *Senior Member, IEEE*

Abstract—Due to the temporal drift of the fiber birefringence in an optical fiber transmission system, the polarization mode dispersion (PMD) effects measured in a time window can be quite different for different time windows of the same duration. Every 10 s for 10 days, the accumulated differential group delay (DGD) was repeatedly measured at 5000 km in a 107-km recirculating loop with loop-synchronous polarization scrambling. In each DGD measurement, the polarization dispersion vector of the 107-km-long fiber was also measured. To model the measured temporal variation of the DGD, two different perturbation algorithms were used to construct random walks through the configuration space of birefringent fibers, where each fiber realization is determined by the standard coarse-step method. With these simulation models, the statistical properties of the spread of the DGD samples over a finite time period were reproduced.

Index Terms—Differential group delay (DGD), fiber drift, optical fiber communication, optical fiber measurement, polarization–mode dispersion (PMD).

I. INTRODUCTION

POLARIZATION mode dispersion (PMD) influences the transmission performance in long-haul optical fiber communication systems and has been studied for more than two decades [1]. Because the effect of PMD varies randomly due to random variations in the fiber birefringence [2], [3], it is important to measure and characterize the probability density functions (pdfs) of random quantities such as the differential group delay (DGD). If the fiber in a straight-line system drifts ergodically over time, which means that over an infinitely long time period, all possible instances of the fiber birefringence are realized with equal probability; then, the resulting pdf of the DGD is Maxwellian [4]. However, any experiment designed to measure the pdf of the DGD must necessarily be undertaken in a finite time window. If the measurement time window T is not long enough, then there can be a large variation between pdfs of the DGD that are measured in different time windows

of duration T. For example, we have observed that, when it is measured over a 3-h time window, the pdf of the DGD at 5000 km in a recirculating loop system can be quite different for different 3-h time windows. Moreover, in some specific windows, the pdf also differs significantly from a modified Bessel function, which describes the long-term DGD pdf in a loop with loop-synchronous polarization scrambling [5]. Consequently, it is important to statistically quantify the extent to which the DGD values spread within a time window of duration T. In this paper, we denote the standard deviation of all DGD samples that are collected in a time window of duration T as $\sigma_\tau(T)$. In the nomenclature of statistical sampling, the quantity $\sigma_\tau(T)$ is also called the spread of the DGD over a time window of duration T. By averaging $\sigma_\tau(T)$ over many different time windows of duration T, we obtain the average spread $\langle\sigma_\tau\rangle(T)$, which statistically quantifies the extent to which the DGD samples are expected to be spread during a time window of duration T. In addition, it is important to measure the extent to which the DGD spread, measured over a time T, varies as the time window changes. Finally, as simulations are widely used to study the system performance, it is also important to develop mathematical models that accurately describe the statistical properties of the spread of the DGD.

A simple dynamical model for the drift in the fiber birefringence over time is a discrete time series of random fiber realizations in which the fiber realization at the next time step is a (small) random perturbation of the current fiber realization. A fiber realization can be characterized by a choice of the birefringence vector as a function of distance along the fiber. This birefringence vector is a real two-vector, whose magnitude equals the birefringence strength and whose direction corresponds to the birefringence orientation. A fiber can be perturbed either by changing the magnitude of the birefringence vector [6], its direction [7], or both as a function of distance.

In general, the fiber birefringence vector at any location drifts randomly over time. Neither the magnitude nor the direction of this drift at any time instant can be predicted without knowing the previous drift history. On the other hand, if the previous drift history is known, one can approximately predict the drift in the next relatively short time period, because the fiber drift remains correlated for some time [8], [9]. Consequently, in order to accurately model the fiber drift, some temporal correlation should be included in the perturbation algorithm. In this paper, we refer to this kind of algorithm as a *quasi-deterministic* model

and the direction in which the birefringence vector drifts as the *drift direction*.

It is difficult, for several reasons, to construct a quasi-deterministic model that exactly models the fiber drift. The measurement of the local fiber birefringence is difficult, and the environmental variations that influence the local fiber birefringence are unpredictable. On the other hand, we will show that it is not necessary to exactly reproduce the fiber birefringence drift in order to study the statistical properties of the DGD spread σ_τ. A quasi-deterministic model with an appropriate amount of temporal correlation will reproduce the measured average spread $\langle \sigma_\tau \rangle(T)$ for almost all values of T, even though the drift of the fiber birefringence in the real system is not exactly reproduced by this model.

We previously mentioned that in a real system, the fiber drift remains correlated for some time. If one repeatedly makes measurements with a sampling interval longer than this correlation time, one would observe an uncorrelated drift process. For example, in an aerial fiber system, where the fiber drift process rapidly decorrelates due to the wind, the correlation time is small compared to typical sampling intervals. Therefore, in this case, a perturbation model in which the magnitude or direction of the perturbation vector field is not correlated from one step to the next accurately describes such observed statistical properties of the fiber drift process as the temporal autocorrelation function (ACF) of the output polarization state and the ACF of the polarization dispersion vector [7]. A perturbation model based on uncorrelated steps also agrees well with the result of a prior experiment in which the polarization state and the DGD were measured with a relatively long sampling interval (~ 2 h) [6]. By analogy to the well-known Brownian motion, in which the direction of a particle's motion at one instant is uncorrelated with the direction at any other instant in time, a model in which the change in the magnitude and the direction of the birefringence vector at each fiber location is uncorrelated from one step to the next is referred to as a Brownian model in this paper. A model with no temporal correlation is easier to implement than a quasi-deterministic model. On the other hand, this model may not accurately reproduce $\langle \sigma_\tau \rangle(T)$ in a system in which the DGD is repeatedly measured with a sampling interval less than the correlation time.

It is useful to compare the models for temporal drift with the models for the spatial variation of the fiber birefringence that have been extensively studied [10]. Two different models have been developed to model the variation of the fiber birefringence with distance, and both of them are accurate in an appropriate parameter range. One model is the fine-step model, in which the fiber birefringence gradually varies over distance: Only after a characteristic length, called the fiber correlation length h, does the birefringence vector become uncorrelated with its value at $z = 0$ [10]. Another model is the coarse-step model, in which the fiber is divided into multiple constant birefringence sections and the birefringence vectors in different sections are uncorrelated [11]. Wai and Menyuk [12] proved that both models yield the same statistical properties for the accumulated DGD as long as the birefringence section length is much longer than the correlation length and the birefringence strength is appropriately scaled. Replacing $\hat{\beta}(z)$ with $d\hat{\beta}/dt$,

where $\hat{\beta}$ represents the local fiber birefringence, the quasi-deterministic model of the temporal fiber drift is analogous to a fine-step model of the spatial variation in the fiber birefringence, and the Brownian model is analogous to a coarse-step model. Thus, it is useful to investigate whether the average spread $\langle \sigma_\tau \rangle(T)$ obtained with the quasi-deterministic model and with the Brownian model also agree when T exceeds an appropriately defined characteristic value.

In order to validate this intuitive picture, we repeatedly measured the DGD at 5000 km in a 107-km recirculating loop system with loop-synchronous polarization scrambling for 10 days with a sampling interval of 10 s to obtain $\langle \sigma_\tau \rangle(T)$. We also measured the polarization dispersion vector $\hat{\Omega}$ of the 107-km loop fiber. Then, we applied the simple Brownian model as well as the quasi-deterministic model to model the temporal drift of the 107-km-long fiber in the loop. In each model, we varied the perturbation parameters and with each choice of the parameters—called a parameter setting in this paper—we perturbed the local fiber birefringence many times to obtain the average spread $\langle \sigma_\tau \rangle(T)$ from the fiber realizations. The simulated average spread $\langle \sigma_\tau \rangle(T)$ was compared with the experimentally measured average spread to evaluate the accuracy of the perturbation model for each parameter setting.

Our study shows that for a time window of duration T longer than a characteristic time, the simple Brownian model agrees well with the experimental results for all settings of the perturbation parameters. This characteristic time, which we called the *correlation time*, is the time duration Δt_0, beyond which the ACF of the temporal variation of $\hat{\Omega}$, $\text{ACF}_d(\Delta t) = \langle (d\hat{\Omega}(t)/dt) \cdot (d\hat{\Omega}(t + \Delta t)/dt) \rangle$, is close to zero. The autocorrelation function ACF_d is different from the ACF of the polarization dispersion vector, $\text{ACF}_s(\Delta t) = \langle \hat{\Omega}(t) \cdot \hat{\Omega}(t + \Delta t) \rangle$, which was the focus of previous studies [6], [7]. The quantity ACF_d characterizes the correlation between the drift directions at different instants in time, while ACF_s describes the correlation between the fiber states at different instants. We also show that when the duration of the time window is shorter than the correlation time, the quasi-deterministic model with an appropriate parameter setting reproduces the value of $\langle \sigma_\tau \rangle(T)$ measured in the experiment, even though the details of the fiber drift may not be exactly reproduced.

In effect, we have developed an approach by which simulation models may be constructed to study the statistical properties of the DGD spread. In this approach, the correlation time Δt_0 of the temporal variation of $\hat{\Omega}$, which is around 25 min in our system, is measured first. If one is only interested in the statistical properties of the DGD spread during a time window longer than the correlation time, a simple Brownian model is sufficient. In such a Brownian model, the perturbation parameter can be arbitrarily chosen within a range for which the amount of the fiber drift in each perturbation step is neither much larger nor much smaller than its value during one sampling interval in the real measurement. By comparison, a quasi-deterministic model with an appropriate parameter setting is accurate for almost any value of T, so that the statistical properties of the DGD spread during a time window shorter than Δt_0 can be characterized. However, this quasi-deterministic model only produces results that agree with the experiment
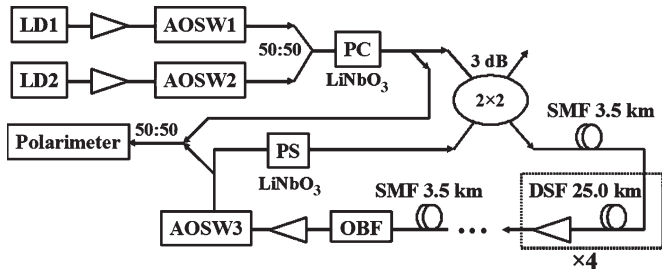
Fig. 1. Experimental setup. LD: laser diode; AOSW: acoustooptic switch; PC: polarization controller; PS: polarization scrambler; SMF: single-mode fiber; DSF: dispersion-shifted fiber; OBF: optical bandpass filter.
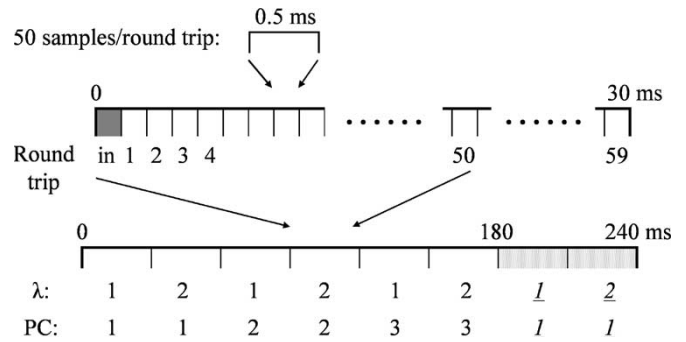

Fig. 2. Chart of the timing history of one DGD measurement. Upper: Fifty samples of Stokes vectors are measured in one round trip, and they are averaged to obtain the Stokes vector for this round trip. Middle: Input polarization state (dark grey filled) and output polarization states at 1–50 round trips are sequentially measured in 30 ms. Data from round trips 51–59 were not used. Lower: Input and output polarization states in six transmitter settings were measured to obtain the DGD value using the JME method. We used an additional 60 ms to remeasure the Stokes vector in the first two settings (light grey filled) in order to estimate the influence of Stokes noise.

when the parameters are properly set. It is not possible to choose the proper parameter setting directly from the experimental data without an accurate measurement of the temporal drift of the local fiber birefringence.

In Section II, we describe the procedure that we used for the 10-day-long experimental measurement of the DGD. We introduce the Brownian model and the quasi-deterministic model in Section III. In Section IV, we compare the long-term pdf of the DGD in these two models with an analytical formula and with the experimental results. From this comparison, we show that in our system, 10 days is almost long enough to accurately determine the statistical properties of the DGD spread. In Section V, we discuss the statistical properties of the DGD spread, and in Section VI, we present our conclusions.

II. EXPERIMENTAL SETUP

In a 107-km recirculating loop system [13], we repeatedly measured the DGD after 50 round trips, which corresponds to approximately 5000 km of propagation, every 10 s for 10 days. As shown in Fig. 1, this loop consists of four spans of dispersion-shifted fiber, each with a length of 25 km, and two spans of standard single-mode fiber, each with a length of 3.5 km. The optical signal loss is compensated by five erbium-doped fiber amplifiers. To reduce the optical noise, we used an in-line optical bandpass filter with a full-width at half-maximum bandwidth of 2.8 nm. The polarization-dependent loss (PDL) was less than 0.5 dB per round trip. To ensure that the loop system emulates the polarization effects in a straight-line system as closely as possible, we used a loop-synchronous LiNbO$_3$ polarization scrambler to randomly rotate the polarization state of the signal once per round trip [14].

At the transmitter, two laser diodes were used to generate two continuous-wave signals at 1551 ± 0.04 nm (10-GHz spacing) that were alternately sent into the loop using two acoustooptic switches. Each signal was transmitted for 30 ms, which is longer than the propagation time for 50 round trips of the loop. Every 60 ms, we made a large change to the input polarization states using a LiNbO$_3$ polarization controller (PC) located immediately prior to the point at which the light is launched into the loop. Thus, within each 180-ms time interval, we launched two wavelengths each with three different polarization states. From the input and output polarization states for these six settings, we calculated the DGD after each of the 50 round trips using the Jones matrix eigenanalysis (JME) method [15]. From

these polarization states, we also calculated the polarization dispersion vector following the procedure in [16].

Fig. 2 shows the timing history of a single DGD measurement. Both the input and output polarization states were measured with a real-time polarimeter (Adaptif Model A1000) at a sampling rate of 100 kHz. Because the light propagation time for one round trip (107 km) was approximately 0.5 ms, we obtained 50 samples per round trip with the 100-kHz sampling rate. We averaged these 50 samples to obtain the Stokes vectors after this round trip. The polarimeter repeatedly sampled the light for 30 ms. This time duration corresponds to 60 round trips, including the input. However, we only kept and analyzed data for the first 50 round trips after the input, so that the total propagation length corresponded approximately to 5000 km. In the first 0.5 ms, one of the two acoustic–optic switches at the transmitter (AOSW1/AOSW2) was on while the other was off so that the signal at one wavelength was loaded into the loop as well as the polarimeter. Because the couplers at the transmitter introduced a negligible amount of DGD, the average of the 50 samples in this 0.5-ms period was used as the input polarization state in the calculation of DGD with no visible loss of accuracy. When both the AOSW1 and AOSW2 were off and the AOSW inside the loop (AOSW3) was on, every group of 50 samples in the complete collection of $50 \times 50 = 2500$ samples was averaged to obtain the polarization state of each round trip. In 30 ms, we captured both the input polarization state and output polarization states at each of the 50 round trips for a given wavelength and for a given input polarization state setting. To obtain the DGD value, one needs to measure input and output polarization states in six transmitter settings—two different wavelengths, each with three different input polarization state settings. By using the AOSWs (AOSW1 and AOSW2) to switch wavelengths and the fast LiNbO$_3$ PC to switch input polarization states, the measurements in the six different settings could be started immediately, one after another. Consequently, we only needed 180 ms (30×6) to finish all six combinations and, thus, one DGD measurement.

As shown in Fig. 2, we set the sampling window to 240 ms. The first 180 ms was used to measure the DGD, as we just described. In the remaining 60 ms (180–240 ms), indicated by the light-grey-filled time slots, we set the transmitter back to the first two settings (0–60 ms) and remeasured the Stokes vectors. Even with the same setting at the transmitter, the results will not be the same as those in 0–60 ms due to Stokes noise, by which we mean the uncertainty in the measurement of the polarization states. This uncertainty is induced by imperfect polarimetry in the instrument, the optical noise, and the fiber drift during one DGD measurement. In earlier work, we have shown that in a long-haul system, the Stokes noise is the major factor limiting the accuracy of the DGD measurement [17]. To estimate its influence on the DGD measurement, we first calculated the noise angle, which we defined to be the angle between the Stokes vector measured during 0–60 ms and the Stokes vector measured during 180–240 ms. On the Poincaré sphere, using the noise angle as the radius, we formed a circle around each of the six output Stokes vectors from the six transmitter settings measured during 0–180 ms. Then, we randomly chose six Stokes vectors from these six circles and used them to recalculate the DGD. The absolute difference between the newly calculated DGD value and the original DGD value gives one sample of the DGD uncertainty. To replicate the random nature of the Stokes noise, we randomly repeated this estimation procedure 25 times for each DGD measurement and thus obtained 25 estimates of the DGD uncertainty. To ensure that the different estimates are statistically independent, the Stokes vectors were chosen randomly on different circles for each estimate in each DGD measurement.

Every 10 s, one DGD sample was obtained for each round trip. At the start of each DGD measurement, the polarization scrambler was reset to generate a new set of random polarization rotations so that in each round trip, the signal underwent an arbitrary polarization rotation that was uncorrelated with the rotations in other round trips and with other DGD measurements. Note that the duration of one DGD measurement was only 180 ms, while resetting the polarization scrambler as well as recording the data from the instrument buffer took about 10 s. For 10 days, we repeated this process continuously and obtained 80 000 DGD samples, except that there was a 12-h gap between the first 50 000 samples and the last 30 000 samples due to an instrument error. During this interval, the system was not touched. For these 80 000 samples, the average DGD after 50 round trips was 4.16 ps, and this value was used in our theoretical studies.

In Fig. 3, we show the complement of the cumulative pdf of the uncertainties in these 80 000 DGD measurements. The total number of uncertainty samples is $25 \times 80\,000$, since we made 25 statistically independent uncertainty estimates for each DGD measurement. With a 99% probability, the DGD measurement uncertainty is less than 1.0 ps at the 50th round trip and is less than 0.2 ps for the 107-km fiber path. The standard deviation of the $25 \times 80\,000$ uncertainty samples at the 50th round trip is around 0.34 ps. Other effects such as higher-order PMD and PDL also affect the measurement. However, our simulation study shows that in the JME method, their effects are negligible if the PDL does not exceed 0.5 dB per round trip [18].
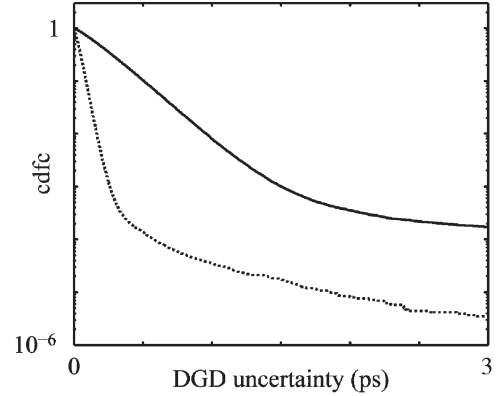

Fig. 3. Complement of the cumulative density function (cdfc) of the uncertainty in the measurement of the DGD in one round trip (dotted line) and of the DGD after 50 round trips (solid line).

To calculate the average spread $\langle \sigma_\tau \rangle(T)$, for a given time window duration T, we divided the 10 days into M nonoverlapping time windows so that $M \times T = 10$ days. We only chose T values such that M is an integer. We calculated $\sigma_\tau(T)$ in each window, and we then averaged $\sigma_\tau(T)$ over all M windows to obtain $\langle \sigma_\tau \rangle(T)$.

In the experiment, we reset the instruments and repeated the DGD measurement every 10 s. To ensure that the calculated value $\sigma_\tau(T)$ is meaningful, we chose the values of T to be greater than 150 s so that the shortest time window contained at least 15 DGD samples. Moreover, to reduce the influence of the measurement uncertainty on the value of $\sigma_\tau(T)$, particularly when T was small and fiber drift was insignificant, we calculated the value of $\sigma_\tau(T)$ in each time window to be $\sigma_\tau(T) = [(\sigma_\tau^{(\mathrm{meas})})^2 - (\sigma_\tau^{(\mathrm{uncertainty})})^2]^{1/2}$, where $\sigma_\tau^{(\mathrm{meas})}$ is the standard deviation of the measured DGD samples, and $\sigma_\tau^{(\mathrm{uncertainty})}$ is the standard deviation of the estimated measurement uncertainties of these DGD samples, which was described earlier in this section.

III. SIMULATION MODELS

We use the coarse-step method to simulate PMD in our system [11]. The 107-km loop fiber is modeled using 75 sections of birefringent fiber, each with a fixed length z and a fixed magnitude of birefringence, expressed as

$$\beta = 2\pi\nu \sqrt{\frac{3\pi}{8 \times 75}} \frac{\langle \tau \rangle}{z} \tag{1}$$

where ν is the optical frequency and where $\langle \tau \rangle$ is the average DGD of the 107-km loop fiber. In the experiment, the polarization scrambler produces a random polarization rotation of the signal once per round trip. In the simulation, this polarization scrambler is modeled by a rotation matrix $\mathsf{R}_{\mathrm{PS}}(i)$ that varied randomly with the round trip number i. Consequently, the polarization transformation matrix for N round trips of the loop is given by

$$\mathsf{R}_N = \prod_{i=1}^{N} \left[\mathsf{R}_{\mathrm{PS}}(i) \prod_{m=1}^{75} e^{\beta z (\hat{\mathbf{r}}_m \times)} \right] \tag{2}$$

where the unit Stokes vector $\hat{\mathbf{r}}_m$ represents the direction of the fiber birefringence in the mth section so that $e^{\beta z(\hat{\mathbf{r}}_m \times)}$ represents the polarization rotation matrix of the mth section of birefringent fiber for an optical signal at frequency ν. The vectors $\hat{\mathbf{r}}_m$ in different sections are uncorrelated. In this work, we assume that the magnitude of the birefringence β does not change over time. Consequently, the fiber realization of the entire system at a given time is determined by $R_{PS}(i)$ and $\hat{\mathbf{r}}_m$. Therefore, the vector $\hat{\mathbf{r}}_m$ also determines the realization of the 107-km length of fiber in the loop, and in this work, it is also referred to as the *state* of the fiber at a given instant. Moreover, at any time instant, the polarization dispersion vector after N round trips $\hat{\boldsymbol{\Omega}}_N$ can be calculated from the transformation matrix R_N as a function of the optical frequency. In this work, we focused on the DGD after N round trips, which is given by the magnitude of $\hat{\boldsymbol{\Omega}}_N$, and the polarization dispersion vector of the 107-km loop fiber $\hat{\boldsymbol{\Omega}}$, which can be calculated from $\hat{\boldsymbol{\Omega}} = R_{PS}(1)^{-1} \times \hat{\boldsymbol{\Omega}}_1$.

The temporal derivative of $\hat{\mathbf{r}}_m$, which represents the variation of the fiber state over time and is referred to as the *drift* of the fiber birefringence in the mth section, is given by

$$\frac{d\hat{\mathbf{r}}_m}{dt} = \phi_r \hat{\mathbf{e}}_{(\hat{\mathbf{p}}_m \times \hat{\mathbf{r}}_m)} \tag{3}$$

where ϕ_r represents the drift rate and the unit Stokes vector $\hat{\mathbf{e}}_{(\hat{\mathbf{p}}_m \times \hat{\mathbf{r}}_m)}$ represents the drift direction, which is determined by the cross product between $\hat{\mathbf{r}}_m$ and a unit vector $\hat{\mathbf{p}}_m$ on the Poincaré sphere. When $\hat{\mathbf{p}}_m$ is constant, as time increases, the vector $\hat{\mathbf{r}}_m$ traces out a circular path on the Poincaré sphere. On the other hand, if the unit vector $\hat{\mathbf{p}}_m$ varies randomly over time, then $\hat{\mathbf{r}}_m$ drifts randomly on the Poincaré sphere. Moreover, when both $\hat{\mathbf{p}}_m$ and ϕ_r are uncorrelated at two instants t_1 and $t_1 + \Delta t$ so that $\langle \hat{\mathbf{p}}_m(t_1) \cdot \hat{\mathbf{p}}_m(t_1 + \Delta t) \rangle_{t_1} = 0$ and $\langle \phi_r(t_1)\phi_r(t_1 + \Delta t) \rangle_{t_1} = 0$, the fiber *drift* is also uncorrelated so that $\langle (d\hat{\mathbf{r}}_m(t_1)/dt) \cdot (d\hat{\mathbf{r}}_m(t_1 + \Delta t)/dt) \rangle_{t_1} = 0$. Note, however, that if the drift rate is small, then the state of the fiber at t_1 and $t_1 + \Delta t$ may still be correlated, i.e., $\langle \hat{\mathbf{r}}_m(t_1) \cdot \hat{\mathbf{r}}_m(t_1 + \Delta t) \rangle_{t_1} \neq 0$.

In Fig. 4, we show the evolution for the first birefringence section $(m = 1)$ of $\hat{\mathbf{r}}_m$ for 800 perturbation steps with the Brownian model and with the quasi-deterministic model. In the Brownian model, at any time instant, the unit vector $\hat{\mathbf{p}}_m$ is uniformly distributed over the full solid angle 4π. The drift rate ϕ_r at different instants is also uncorrelated, and at each instant, ϕ_r is Gaussian distributed with zero mean and a standard deviation σ_{ϕ_r}. Consequently, in the Brownian model, one only needs to set the standard deviation of the drift rate ϕ_r, and for the 800 perturbations shown in Fig. 4(a), $\sigma_{\phi_r} = 0.01$ rad. As shown in Fig. 4(a), the vector $\hat{\mathbf{r}}_m$ drifts in any direction on the Poincaré sphere with equal probability, and the drift of the fiber $d\hat{\mathbf{r}}_m/dt$ at any two instants is uncorrelated. However, as we mentioned earlier, the state of the fiber $\hat{\mathbf{r}}_m$ may remain correlated for a certain length of time. For example, in Fig. 4(a), the vectors $\hat{\mathbf{r}}_m$ all lie within a small region of the Poincaré sphere.

In the quasi-deterministic model, instead of being at an arbitrary position on the Poincaré sphere at any instant, the unit
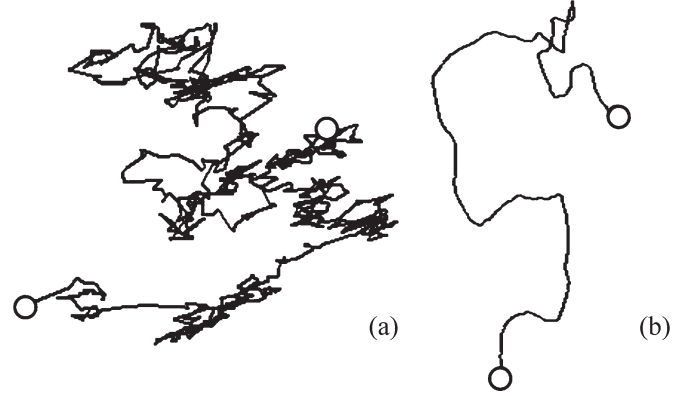

Fig. 4. Evolution of $\hat{\mathbf{r}}_1$ for 800 perturbation steps (a) with the Brownian model and (b) with the quasi-deterministic model. We show the evolution by projecting a small region of the Poincaré sphere onto a plane. The angle between the original $\hat{\mathbf{r}}_1$ and $\hat{\mathbf{r}}_1$ after 800 perturbations steps (both marked by circles) is (a) 0.26 rad in the Brownian model and (b) 0.09 rad in the quasi-deterministic model.

vector $\hat{\mathbf{p}}_m$ changes more gradually over time, i.e., it traces out a Brownian-motion-like path, similar to the one traced out by the vector $\hat{\mathbf{r}}_m$ in the Brownian model. The standard deviation of the drift rate of $\hat{\mathbf{p}}_m$ is denoted by σ_{ϕ_p}, which statistically determines the rate at which the drift *direction* of $\hat{\mathbf{r}}_m$ varies. In this model, the drift rate of $\hat{\mathbf{r}}_m$ itself ϕ_r is held fixed. Thus, the random properties of the fiber drift in the quasi-deterministic model is determined by two parameters, namely 1) σ_{ϕ_p} and 2) ϕ_r. Fig. 4(b) shows $\hat{\mathbf{r}}_1$ in 800 perturbation steps with the quasi-deterministic model when $\sigma_{\phi_p} = 0.2$ rad and $\phi_r = 0.0005$ rad. Since the vector $\hat{\mathbf{p}}_m$ remains correlated for a certain amount of time, the *drift* $d\hat{\mathbf{r}}_m/dt$ of the mth section preserves a certain degree of correlation during this correlation time.

In the simulation, the quantity σ_{ϕ_r} in the Brownian model is the standard deviation of the amount by which $\hat{\mathbf{r}}_m$ is perturbed in each step. In the quasi-deterministic model, σ_{ϕ_p} is the standard deviation of the perturbation amount of $\hat{\mathbf{p}}_m$ in one step and ϕ_r is the fixed perturbation amount of $\hat{\mathbf{r}}_m$ per step. In this paper, we chose different values for these perturbation parameters, and for each such *parameter setting*, we perturbed $\hat{\mathbf{r}}_m$ six million times. For each parameter setting, we also divided the six million perturbations into M perturbation windows, each with n perturbation steps so that $M \times n = 6 \times 10^6$, and we calculated $\langle \sigma_\tau \rangle(n)$ as a function of n for $n > 15$ following the same procedure that we used in the experiment. However, in the simulation, σ_τ is not influenced by the Stokes noise and is therefore directly calculated from the standard deviation of the DGD samples in each perturbation window.

Each perturbation step corresponds to an elapsed time period in the experiment, $t_{\text{perturbation}}$, during which the fiber realization drifts slightly. Thus, when the value of $t_{\text{perturbation}}$ is determined, $\langle \sigma_\tau \rangle(n)$ is converted to $\langle \sigma_\tau \rangle(T)$ using $T = n t_{\text{perturbation}}$, which is then compared with $\langle \sigma_\tau \rangle(T)$ measured in the experiment. Because we estimated the statistics of the DGD using only a finite number of samples in both the experiment and the simulations, there is an uncertainty in the average value $\langle \tau \rangle$ of all the DGD samples, and hence in the estimated values of the average spread $\langle \sigma_\tau \rangle(T)$. To reduce the influence of this uncertainty, we divided the average spread $\langle \sigma_\tau \rangle(T)$ by the

TABLE I
PARAMETER SETTING, PERTURBATION STEP TIME, AND AVERAGE DGD AT THE 50TH ROUND TRIP IN
THE BROWNIAN MODEL AND IN THE QUASI-DETERMINISTIC MODEL (QUASI-D)

setting	$\sigma_{\phi r}$ (rad)	$\sigma_{\phi p}$ (rad)	ϕ_r (rad)	$t_{\text{perturbation}}$ (seconds)	$\langle \tau_{50} \rangle$ (ps)
Brownian 1	0.005	–	–	8.4	4.05
Brownian 2	0.010	–	–	32.2	4.13
Brownian 3	0.020	–	–	122.9	4.20
Quasi-D 1	–	0.1	0.0005	9.7	4.14
Quasi-D 2	–	0.2	0.0005	4.8	4.17
Quasi-D 3	–	0.2	0.0010	16.0	4.16

average of all DGD samples in the long-term measurement or in the long-term simulation of the fiber drift. We call the resulting value $\langle \sigma_\tau \rangle_{\text{nor}}(T) = \langle \sigma_\tau \rangle (T)/\langle \tau \rangle$ the normalized average spread of the DGD. In the remainder of the paper, we compare the values of $\langle \sigma_\tau \rangle_{\text{nor}}(T)$ in the experiment with those obtained using simulations. For each parameter setting, we tried different values of $t_{\text{perturbation}}$, and we chose the one that minimizes the average absolute difference between the experimental and simulated functions $\langle \sigma_\tau \rangle_{\text{nor}}(T)$, i.e., we minimized $\int |\langle \sigma_\tau \rangle_{\text{nor,experiment}}(T) - \langle \sigma_\tau \rangle_{\text{nor,simulation}}(T)|dT$.

The value of $t_{\text{perturbation}}$ is influenced by the perturbation parameters and the number of birefringent sections used to model a given length of the fiber path, which, in this paper, is 75 sections for the 107-km loop fiber. Conversely, for any combination of the perturbation parameters and for any number of birefringent sections that is greater than 10 [12], the value of $t_{\text{perturbation}}$ that minimizes the average absolute difference between the normalized average spreads in the experiment and simulation results in a good fit between these two curves. However, there is no guarantee that the two $\langle \sigma_\tau \rangle_{\text{nor}}(T)$ curves agree at every value of T, or even every T within the range of interest, since the simulation may not accurately describe the statistical properties of the DGD spread in the experiment.

In this work, we used three different parameter settings for the Brownian model and another three different parameter settings for the quasi-deterministic model. The perturbation parameters and the corresponding values of $t_{\text{perturbation}}$ chosen for these settings are listed in Table I. The average DGD at the 50th round trip for the six million DGD samples in each setting is also given and is the value we used to calculate $\langle \sigma_\tau \rangle_{\text{nor}}(T)$ from $\langle \sigma_\tau \rangle (T)$. As shown in the table, when $\sigma_{\phi r}$ or ϕ_r increases, the vector $\hat{\mathbf{r}}_m$ is perturbed on average by a larger amount in each step, so that each perturbation step corresponds to a longer drift time in the experiment. By contrast, as $\sigma_{\phi p}$ increases, $t_{\text{perturbation}}$ decreases, because the drift of $\hat{\mathbf{r}}_m$ is less correlated from step to step. This behavior is analogous to the movement of a particle. For a given velocity, if the particle moves in a random direction at any instant, the overall displacement during a given time interval will be less than that if the particle moves in a straight line.

In principle, one can vary the values of the perturbation parameters in a range different from that in Table I. The range

of variation in this paper was chosen so that $t_{\text{perturbation}}$ is not significantly different from the measurement interval of 10 s and so that the values of the normalized average spread of the DGD, $\langle \sigma_\tau \rangle_{\text{nor}}(T)$, in the simulation can be compared to those in the experiment over as wide a range of T as possible.

The birefringence vector of each fiber section $\hat{\mathbf{r}}_m$ in these six million realizations is uniformly distributed on the Poincaré sphere, which indicates that the fiber drifts ergodically in both models. In each perturbation, we also randomly varied $\mathsf{R}_{\text{PS}}(i)$ to emulate a different setting of the polarization scrambler for each different measurement.

IV. PDF OF DGD DURING THE 10 DAYS AND IN SIX MILLION FIBER REALIZATIONS

Every measurement is performed during a finite time window. In order to accurately characterize the statistical properties of the spread of the DGD, this time window should be relatively long. In this work, we compared the pdf of the DGD measured over 10 days to that obtained numerically from six million perturbations and to an analytical formula for the pdf of the DGD [5]. This analytical formula describes the pdf of the DGD in a recirculating loop with loop-synchronous polarization scrambling in the case that the samples are collected over an infinitely long time period [19]. The formula for the pdf of the DGD, x, after N round trips of a loop with an average DGD $\langle \tau_N \rangle$, is given by [5]

$$F(x; \langle \tau_N \rangle) = \left(\frac{1024 x^2}{\pi^4 \langle \tau_N \rangle^3} \right) K_0 \left(\frac{8x}{\pi \langle \tau_N \rangle} \right) \qquad (4)$$

where K_0 is the zeroth-order modified Bessel function of the second kind. The average DGD after N round trips is related to the average DGD per round trip $\langle \tau \rangle$ by $\langle \tau_N \rangle = \sqrt{8N/3\pi} \langle \tau \rangle$. In the simulation, we used (1) to determine β from $\langle \tau \rangle$, where the value of $\langle \tau \rangle$ was calculated from the measured value of $\langle \tau_N \rangle$. The values of $\langle \tau_N \rangle$ in both the simulation and in the analytical formula are set to the value obtained in the experiment: $\langle \tau_{50} \rangle = 4.16$ ps.

The pdf in (4) is not Maxwellian, which describes the pdf of DGD in a straight-line system in some limits [4]. In a
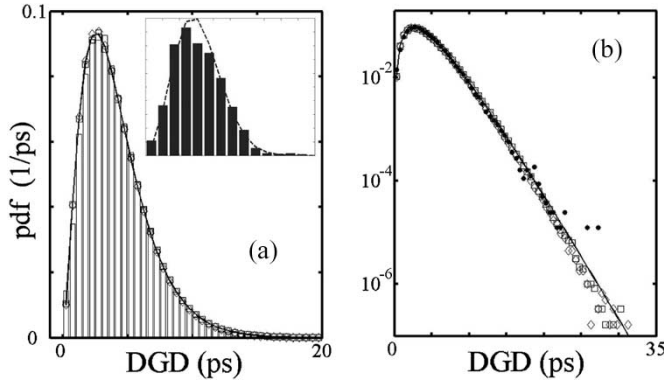
Fig. 5. PDF of the DGD after the 50th round trip (a) on a linear scale and (b) on a logarithmic scale, obtained from the 10-day measurement (bars on the linear scale and dots on the logarithmic scale), from the Brownian model (open diamonds), from the quasi-deterministic model (open squares), and from the analytical formula with $\langle \tau_{50} \rangle = 4.16$ ps (solid line). Note that on the linear scale, the tail of the pdf for the DGD values larger than 20 ps is not shown. The inset in (a) shows the pdf of DGD of the 107-km loop fiber during the 10 days (bar) and, we compare it with the Maxwellian distribution (dashed curve). The maximal x-value of the inset is 2.0 ps.

recirculating loop, the measured DGD values at different times are different due to two factors. First, the loop-synchronous polarization scrambler settings vary randomly between measurements. Second, the birefringence of the loop fiber drifts randomly over time. If one does not consider the loop fiber drift, then the DGD per round trip is constant and the pdf of the DGD after N round trips will be approximately Maxwellian [14]. However, fiber drift is inevitable. When the loop fiber drifts ergodically, one would observe a Maxwellian distribution [4] of the pdf of the DGD measured after one round trip when the data is collected for the DGD over many round trips for a long time period. The Maxwellian pdf of the DGD in each round trip, together with the Maxwellian conditional pdf of the accumulated DGD with $N \gg 1$ round trips for a given DGD per round trip, then yields the pdf of the DGD described by (4).

Fig. 5 shows the pdf of the DGD in our system at the 50th round trip on both (a) a linear and (b) a logarithmic scale from the 80 000 measurements during 10 days. We show the results from the two models, each with six million perturbation steps and from the analytical formula (4). As shown in the figure, the experimentally measured pdf of the DGD agrees well with the analytical formula (4) for all DGD values up to 20 ps. The probability that the DGD is larger than 20 ps is approximately 1.9×10^{-4}. Because of this low probability, there is an insufficient number of experimental DGD samples in this region and a slight discrepancy appears. For all settings listed in Table I, the pdf of the DGD agrees well with the analytical formula (4) up to 25 ps. Here, we only show the pdf of the DGD for setting 2 with the Brownian model and for setting 2 with the quasi-deterministic model, but the agreement is equally good for the other settings. Despite this good agreement of the pdfs, we will show in the next section that there is still a slight discrepancy in the DGD spread even after 10 days, and we will estimate the additional time required to eliminate this discrepancy.

V. DGD Spread in Finite Time Windows

A. ACF of the Polarization Dispersion Vector

An important property of the Brownian model that we use in this paper is that from one perturbation step to the next, there is no correlation between the *directions* in which the state $\hat{\mathbf{r}}_m$ of the fiber drifts. However, in a real fiber transmission system, these drift directions may well be correlated for a time, which we refer to as the correlation time of the fiber drift $d\hat{\mathbf{r}}_m/dt$. Because $\hat{\mathbf{r}}_m$ determines the polarization dispersion vector $\hat{\boldsymbol{\Omega}}$ of the loop fiber, the evolution of $\hat{\boldsymbol{\Omega}}$ in a real system can therefore be different from that in the Brownian model.

On the other hand, under certain circumstances, the Brownian model can still accurately describe the observed statistical properties of the effects due to PMD in such systems. For example, if the correlation time of $d\hat{\mathbf{r}}_m/dt$ is shorter than the sampling interval in a temporal series of measurements of $\hat{\mathbf{r}}_m$, one would expect the fiber drift directions to be uncorrelated so that the system could be accurately described by the Brownian model. In the study of the DGD spread, we also expect that when the duration of the time window T is larger than a certain value, the value of $\langle \sigma_\tau \rangle_{\mathrm{nor}}(T)$ obtained with the Brownian model would also agree with the experimental value. Moreover, this value of T should be related to the time length beyond which $d\hat{\boldsymbol{\Omega}}/dt$ becomes uncorrelated, because if one considers many nonoverlapping time windows, each with a duration longer than this time length, the temporal evolution of $\hat{\boldsymbol{\Omega}}$ in two different windows is uncorrelated, as is the case in the Brownian model.

Thus, in this study of DGD spread, we focused on the temporal ACF of the time derivative of polarization dispersion vector $\mathrm{ACF}_d(\Delta t)$, which quantifies the degree of correlation between the temporal variation of $\hat{\boldsymbol{\Omega}}$ at t and $t + \Delta t$ and is defined by

$$\mathrm{ACF}_d(\Delta t) = \left\langle \frac{d\hat{\boldsymbol{\Omega}}(t)}{dt} \cdot \frac{d\hat{\boldsymbol{\Omega}}(t + \Delta t)}{dt} \right\rangle_t. \qquad (5)$$

In a loop system with loop-synchronous polarization scrambling, the polarization dispersion vector after multiple round trips of the loop will be decorrelated for any two different samples by the polarization scrambler, since we randomly change the setting of the polarization scrambler from sample to sample. Therefore, in this paper, we focus on ACF_d for the polarization dispersion vector of the 107-km straight-line fiber in the loop, which is not changed by the repeated resetting of the polarization scrambler, as shown in Fig. 1. In Fig. 6(a), we show $\mathrm{ACF}_d(\Delta t)$ in the simulation, and in Fig. 6(b), we show $\mathrm{ACF}_d(\Delta t)$ measured for the 107-km loop fiber. In the Brownian model, ACF_d is close to zero for all values of $\Delta t > t_{\mathrm{perturbation}}$, while in the quasi-deterministic model, ACF_d is larger than zero when Δt is less than 30, 12, and 21 min with settings 1–3, respectively. Due to the correlated drift of $\hat{\mathbf{r}}_m$ in this model, the temporal variation of $\hat{\boldsymbol{\Omega}}$ is strongly correlated when Δt is small. As Δt increases, the drift of $\hat{\mathbf{r}}_m$ becomes less correlated. Therefore, the temporal variation of $\hat{\boldsymbol{\Omega}}$ also becomes less correlated and ACF_d approaches zero.
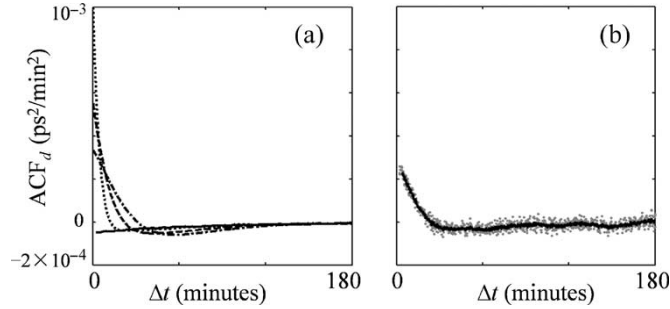
Fig. 6. (a) $\text{ACF}_d(\Delta t)$ for setting 3 in the Brownian model (solid line) and for settings 1–3 in the quasi-deterministic model (1: dot-dashed line; 2: dotted line; 3: dashed line). (b) Measured $\text{ACF}_d(\Delta t)$ for the 107-km loop fiber for two different choice of the differential δt used to estimate the derivative: 2 min (lighter dots); and 4 min (darker dots).

Fig. 6(b) shows that the temporal variation of $\hat{\Omega}$ in the experiment is correlated and ACF_d is positive when Δt is less than 25 min. Consequently, the fiber drift in the loop system does show some degree of correlation. This experimentally observed behavior is similar to the behavior in the quasi-deterministic model. Note that in the experiment, the temporal derivative in (5) was estimated by taking a small time difference δt and dividing the difference between the vectors $\hat{\Omega}(t)$ and $\hat{\Omega}(t + \delta t)$ by δt. In comparison to the measurement of DGD, the measurement of $\hat{\Omega}$ is more sensitive to the factors such as PDL, noise, and fiber drift within the 180-ms time of a DGD measurement. Thus, the differential step δt should be relatively large so that the evolution dominates the measurement uncertainty. As shown in the figure, $\text{ACF}_d(\Delta t)$ is smoother with $\delta t = 4$ min than with $\delta t = 2$ min, because the uncertainty in each $\hat{\Omega}$ measurement is insignificant when compared to the drift-induced $\hat{\Omega}$ variation during $\delta t = 4$ min.

Since the measured $\text{ACF}_d(\Delta t)$ is close to zero after 25 min, there is only a weak correlation between the temporal variation in $\hat{\Omega}$ at two times that at more than 25 min apart. Thus, we might anticipate that $\langle \sigma_\tau \rangle_{\text{nor}}(T)$ obtained with the Brownian model and in the experiment will be in close agreement when $T > 25$ min.

The auto-correlation function ACF_d is related to ACF_s by

$$\text{ACF}_d(\Delta t) = -\frac{d^2 [\text{ACF}_s(\Delta t)]}{d(\Delta t)^2}. \tag{6}$$

Here, $\text{ACF}_s(\Delta t) = \langle \hat{\Omega}(t) \cdot \hat{\Omega}(t + \Delta t) \rangle$ is the ACF of the state of the fiber, which has been used to characterize the temporal drift of the fiber [6], [7]. Thus, a measurement of $\text{ACF}_s(\Delta t)$ can also be used to determine $\text{ACF}_d(\Delta t)$. However, since $\text{ACF}_s(\Delta t)$ only describes the correlation of the $\hat{\Omega}$ states at two instants, it does not directly characterize the drift process itself. Moreover, the correlation time associated with the $\text{ACF}_s(\Delta t)$ in previous work [6] and the correlation time associated with $\text{ACF}_d(\Delta t)$ in this work describe different drift properties. The correlation time associated with $\text{ACF}_s(\Delta t)$ describes how fast the fiber drifts away from its original state, but in this work, the correlation time of 25 min, which is associated with $\text{ACF}_d(\Delta t)$, describes how fast the fiber drift direction becomes decorrelated.

Between 25 and 100 min, the temporal variation of $\hat{\Omega}$ is weakly correlated, rather than fully uncorrelated, because $\text{ACF}_d(\Delta t)$ is slightly negative. Similarly in the Brownian model, even though the direction of birefringence vector $\hat{\mathbf{r}}_m$ is arbitrarily perturbed so that $\langle (d\hat{\mathbf{r}}_m(t)/dt) \cdot (d\hat{\mathbf{r}}_m(t + \Delta t)/dt) \rangle = 0$ for all values of $\Delta t > t_{\text{perturbation}}$, ACF_d is also slightly negative when Δt is less than 100 min, as shown in Fig. 6(a). Nevertheless, the correlation is weak when compared with times for which $\text{ACF}_d(\Delta t) > 0$. Hence, we refer to the smallest positive time Δt_0 for which $\text{ACF}_d(\Delta t_0) = 0$ as the *correlation time* of the temporal variation of $\hat{\Omega}$.

B. Average Spread of the DGD $\langle \sigma_\tau \rangle(T)$ in the Brownian Model

We now investigate the accuracy of the Brownian model. In Fig. 7, we show $\langle \sigma_\tau \rangle_{\text{nor}}(T)$ as a function of T in the experiment and in the Brownian model with the three different settings of σ_{ϕ_r} listed in Table I. We display $\langle \sigma_\tau \rangle_{\text{nor}}(T)$ with T on a logarithmic scale. As described earlier, we choose the value of $t_{\text{perturbation}}$ so as to minimize the integral of the difference between the experimental curve and the numerical curve. This procedure is equivalent to horizontally shifting $\langle \sigma_\tau \rangle_{\text{nor}}(T)$ in the simulation in Fig. 7 back and forth until at some value of $t_{\text{perturbation}}$, the experimental curve and the simulation curve have a minimal average vertical difference.

As shown in Fig. 7, when the duration T is longer than 25 min, which is the correlation time Δt_0 of the temporal variation of $\hat{\Omega}$ for the 107-km loop fiber, all three simulation curves agree well with the experimental result. Therefore, even though the Brownian model may not describe the exact way in which the fiber drifts, it is sufficient for a study of the statistical properties of the DGD spread during a time window with a duration T that is greater than the correlation time of the temporal variation of $\hat{\Omega}$.

In a recirculating loop with loop-synchronous polarization scrambling, the spread of the DGD samples during one time window is caused by the fiber drift as well as by the loop-synchronous polarization scrambler, which randomly varies in a different DGD measurement (10 s) in our experiment and every perturbation step ($t_{\text{perturbation}}$) in the simulations. For a time window that is short enough so that the fiber drift is insignificant but is also long enough so that many measurements could be taken during the window ($T \gg 10$ s), the pdf of the DGD would approach a Maxwellian distribution, which describes the pdf of the DGD for a given DGD per round trip. When the time window is long enough so that the fiber drift and thus the variation of DGD per round trip becomes significant, the spread of the pdf of the DGD at the 50th round trip is greater than that of the Maxwellian distribution with the same mean. The pdf approaches the analytical formula (4) when the time window becomes sufficiently long and the fiber drift in each measurement window is large enough so that the DGD per round trip is nearly Maxwellian distributed. Consequently, as shown in Fig. 7, when T is small, $\langle \sigma_\tau \rangle_{\text{nor}}$ approaches 0.41, which is the value of $\langle \sigma_\tau \rangle_{\text{nor}}$ for the Maxwellian distribution with a mean of $\langle \tau_{50} \rangle = 4.16$ ps. When the duration T increases, we find that $\langle \sigma_\tau \rangle_{\text{nor}}$ increases. When $T > 1000$ h, we find
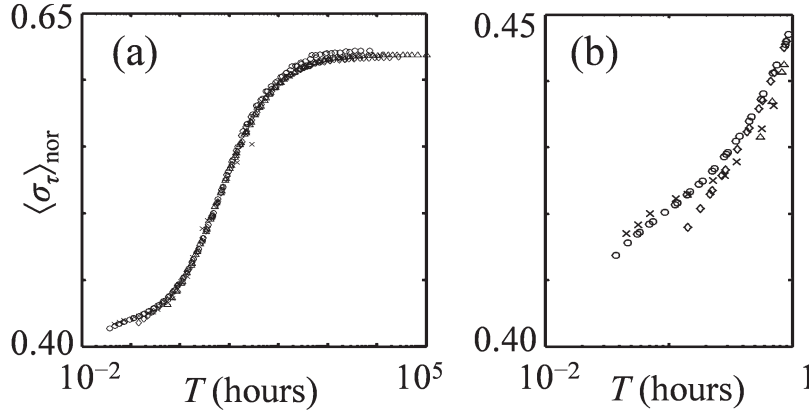
Fig. 7.   Normalized average spread $\langle\sigma_\tau\rangle_{\mathrm{nor}}$ of DGD as a function of the duration of a time window T, in the experiment (crosses), and in the Brownian model with the three different settings that were listed in Table I: setting 1 (open circles); setting 2 (open diamonds); and setting 3 (open triangles). In (b), we have enlarged the portion of (a) in which $T < 1$ h.
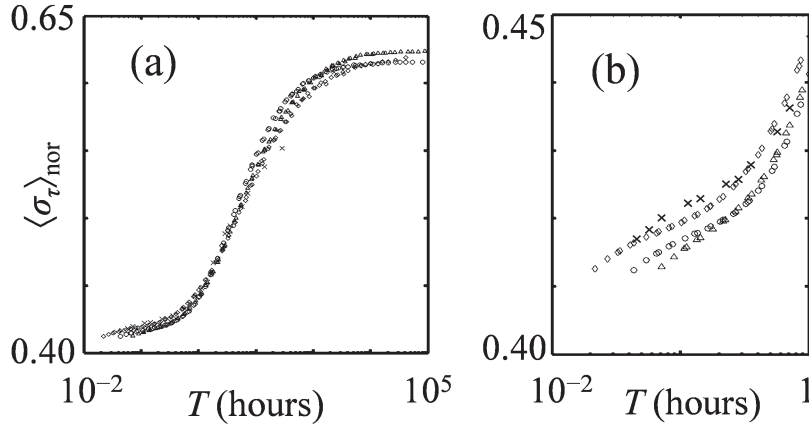

Fig. 8.   Normalized average spread $\langle\sigma_\tau\rangle_{\mathrm{nor}}$ of DGD as a function of the duration of a time window T in the experiment (crosses) and in the quasi-deterministic model with the three different settings that were listed in Table I: setting 1 (open circles); setting 2 (open diamonds); and setting 3 (open triangles). In (b), we have enlarged the portion of (a) in which $T < 1$ h.

that $\langle\sigma_\tau\rangle_{\mathrm{nor}}$ approaches 0.62, which is the value of $\langle\sigma_\tau\rangle_{\mathrm{nor}}$ for the pdf given by the analytical formula (4). Consequently, for the system that we studied, a time window of 1000 h (= 42 days) should be sufficiently long for the DGD statistics to approach those that would be collected over an infinite time period. Although the pdf of the DGD resembles the analytical formula (4), a 10-day measurement is still not sufficiently long, and the pdf of the DGD in another 10 days might be slightly different.

C. Average Spread of the DGD $\langle\sigma_\tau\rangle(T)$ in the Quasi-Deterministic Model

In Fig. 7, we show that when T is less than 25 min, the Brownian model deviates from the experimental results. In this short time duration, the variation of $\hat{\Omega}$ in neighboring time windows is correlated, and so the evolution of $\langle\sigma_\tau\rangle_{\mathrm{nor}}$ with T is different from that in the Brownian model.

It is difficult to find a model that exactly reproduces the drift of the fiber realization, because it is not possible to accurately monitor the drift of the local birefringence in a long-haul system. Recently, a reflectometric method was reported to measure the local birefringence in a fiber path whose length is in tens of kilometers [20]. However, this method cannot

be applied to a long-term continuous monitoring of the local fiber birefringence in a relatively long transmission system. Nonetheless, we will show that the quasi-deterministic model may still reproduce $\langle\sigma_\tau\rangle(T)$ in a real system with gradual fiber drift.

In Fig. 8, we show $\langle\sigma_\tau\rangle_{\mathrm{nor}}(T)$ in the experiment and in the quasi-deterministic model with the three parameter settings listed in Table I. With all three settings, we find that $\langle\sigma_\tau\rangle_{\mathrm{nor}}(T)$ also converges to the experimental results when T is greater than 30 min. As shown in Fig. 6, $\mathrm{ACF}_d(\Delta t)$ is close to zero with all three settings as well as in the experiment when Δt is greater than 30 min. Consequently, when T is greater than 30 min, the values of $\langle\sigma_\tau\rangle_{\mathrm{nor}}(T)$ obtained with all three settings and from the experiment all agree well with those obtained using the Brownian model. In setting 2, we find that $\langle\sigma_\tau\rangle_{\mathrm{nor}}(T)$ agrees well with the experimental result over almost the whole range of T. Therefore, with an appropriate choice of parameters, the quasi-deterministic model can accurately describe $\langle\sigma_\tau\rangle_{\mathrm{nor}}(T)$ in a real system.

As discussed earlier, the Brownian and quasi-deterministic models are analogous to the coarse-step and fine-step models, which are used to model the random spatial variation of the fiber birefringence. For a length longer than the correlation length h, the coarse-step model is accurate. By analogy, for a time
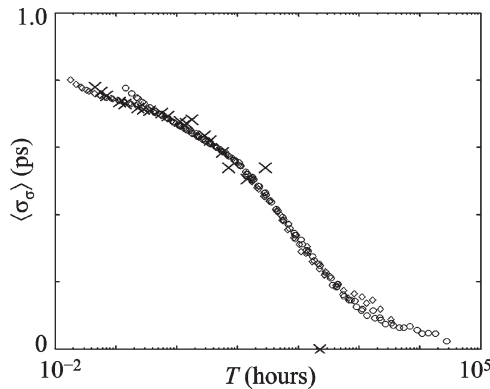
Fig. 9. Second moment $\sigma_\sigma(T)$ of the standard deviation of the DGD measured in a time window of duration T, versus T, in the experiment (crosses), in the Brownian model with setting 2 (open circles), and in the quasi-deterministic model with setting 2 (open diamonds).

window longer than the correlation time Δt_0 of the temporal variation of $\hat{\mathbf{\Omega}}$, our results show that the Brownian model is also accurate. In order to accurately calculate the statistical properties of the DGD in a fiber shorter than h, we require a model for how the fiber birefringence gradually evolves with distance. Such a model is given by an appropriate fine-step model. Similarly, in the study of the DGD spread in a time window, with an appropriate choice of parameter, the quasi-deterministic model can be accurate for almost any duration T.

D. Second Moment of $\sigma_\tau(T)$

We also studied the second moment, $\sigma_\sigma(T) = \sigma_{\sigma_\tau}(T)$, of the standard deviation of the DGD in a time window of duration T, $\sigma_\tau(T)$, where as before the samples were collected over all time windows of duration T. This quantity measures the extent to which the width of the pdf of the DGD varies in different time windows of duration T.

In Fig. 9, we show $\sigma_\sigma(T)$ in the experiment, in the Brownian model, and in the quasi-deterministic model. As in the case of $\langle\sigma_\tau\rangle_{\text{nor}}(T)$, the quasi-deterministic model with setting 2 agrees with the experimental result over a wide range of values of T, and the Brownian model is accurate when T is greater than 25 min.

When measured over very long time windows, the pdf of the DGD closely resembles the pdf measured over an infinitely long duration that is given by the analytical formula (4) in the case of a recirculating loop with polarization scrambling or by a Maxwellian function in the case of a straight-line system. Consequently, as T increases, the values of $\sigma_\sigma(T)$ measured in different windows of duration T become closer to each other, and so, $\sigma_\sigma(T)$ decreases. When $T = 1000$ h (42 days), σ_σ is less than 0.1 ps, which is less than 2.5% of the average DGD of 4.16 ps. Therefore, in different time windows of this duration, one would observe almost identical DGD statistics.

When we compare $\sigma_\sigma(T)$ in the experiment and in the simulation, the perturbation time step $t_{\text{perturbation}}$ was determined by minimizing the average absolute difference between $\sigma_\sigma(T)$ in the experiment and $\sigma_\sigma(T)$ in the simulation. The values that we obtained were $t_{\text{perturbation}} = 32.6$ s for

setting 2 with the Brownian model and $t_{\text{perturbation}} = 4.0$ s for setting 2 with the quasi-deterministic model. By comparison, when we minimize the difference between $\langle\sigma_\tau\rangle_{\text{nor}}(T)$ in the experiment and $\langle\sigma_\tau\rangle_{\text{nor}}(T)$ in the simulation, $t_{\text{perturbation}} = 32.2$ s for setting 2 with the Brownian model and $t_{\text{perturbation}} = 4.8$ s for setting 2 with the quasi-deterministic model. We found that there is about a 30% discrepancy in the value of $t_{\text{perturbation}}$ for a given setting. This discrepancy occurs, because the experimental measurement lasted for 10 days, which is not sufficiently long. Nevertheless, in comparison with the whole range of T (seven orders of magnitude), a horizontal shift of the simulation curves by 30% is slight.

VI. Conclusion

We used the average spread of the DGD during a time window of duration T, $\langle\sigma_\tau\rangle(T)$, to quantify the pdf of the DGD measured during a time window of duration T, which is directly related to the variation of the system performance during a finite time window. A systematic approach was developed to construct temporal fiber drift models that accurately reproduce $\langle\sigma_\tau\rangle(T)$ in the real system. In this approach, the ACF of the temporal variation of $\hat{\mathbf{\Omega}}$, $\text{ACF}_d(\Delta t)$, was measured to obtain the correlation time Δt_0, beyond which $\text{ACF}_d(\Delta t)$ is close to zero. The average DGD spread $\langle\sigma_\tau\rangle(T)$ in a time window of duration T longer than Δt_0 can be accurately modeled by a simple Brownian model with any setting of the perturbation parameters. By comparison, the quasi-deterministic model, with an appropriate degree of correlation, accurately reproduces $\langle\sigma_\tau\rangle(T)$ for almost all values of T. However, the quasi-deterministic model requires a specific parameter choice to match the experiments.

We applied this approach to the 107-km straight-line fiber in a recirculating loop, and we compared the experimental results and the simulation results for $\langle\sigma_\tau\rangle(T)$ at 5000 km, which corresponds to 50 round trips in the 107-km loop fiber. The correlation time of the 107-km loop fiber is approximately 25 min. The measured average spread $\langle\sigma_\tau\rangle(T)$ is accurately described by the Brownian model when T is longer than 25 min, while for a time window of almost arbitrary duration, with a proper choice of parameters, the quasi-deterministic model can accurately reproduce the experimental results. Consequently, with this approach, we developed fiber drift models with which $\langle\sigma_\tau\rangle(T)$ can be accurately studied. Other effects such as nonlinearity and noise can be incorporated in these models to study the temporal variation of the system performance.

References

[1] H. Kogelnik, R. M. Jopson, and L. E. Nelson, "Polarization-mode dispersion," in *Optical Fiber Telecommunications*, vol. IVB, I. P. Kaminow and T. Li, Eds. San Diego, CA: Academic, 2002, ch. 15, pp. 725–861.

[2] R. A. Harmon, "Polarization stability in long lengths of monomode-fibre," *Electron. Lett.*, vol. 18, no. 24, pp. 1058–1060, 1982.

[3] G. J. Foschini and C. D. Poole, "Statistical theory of polarization dispersion in single mode fiber," *J. Lightw. Technol.*, vol. 9, no. 11, pp. 1439–1456, Nov. 1991.

[4] F. Curti, B. Daino, Q. Mao, F. Matera, and C. G. Someda, "Statistical treatment of the evolution of the principle states of polarization in single-mode fiber," *J. Lightw. Technol.*, vol. 8, no. 8, pp. 1162–1165, Aug. 1990.

[5] H. Xu, B. S. Marks, J. Zweck, L. Yan, C. R. Menyuk, and G. M. Carter, "The long-term distribution of differential group delay in a recirculating

loop," in *Proc. Symp. Optical Fiber Measurements*, Boulder, CO, Sep. 2004, pp. 95–98.

[6] M. Karlsson, J. Brentel, and P. A. Andrekson, "Long-term measurement of PMD and polarization drift in installed fiber," *J. Lightw. Technol.*, vol. 18, no. 7, pp. 941–951, Jul. 2000.

[7] D. S. Waddy, L. Chen, and X. Bao, "Theoretical and experimental study of the dynamics of polarization-mode dispersion," *IEEE Photon. Technol. Lett.*, vol. 14, no. 4, pp. 468–470, Apr. 2002.

[8] C. D. Angelis, A. Galtarossa, G. Gianello, F. Matera, and M. Schiano, "Time evolution of polarization mode dispersion in long terrestrial links," *J. Lightw. Technol.*, vol. 10, no. 5, pp. 552–555, May 1992.

[9] M. Brodsky, M. Boroditsky, P. Magill, N. J. Frigo, and M. Tur, "Field PMD measurements through a commercial, Raman-amplified ULH transmission system," in *Proc. LEOS Polarization Mode Dispersion (PMD) Summer Topical Meeting*, Vancouver, BC, Canada, Jul. 2003, pp. MB3.3/15–MB3.3/16.

[10] I. P. Kaminow, "Polarization in optical fibers," *IEEE J. Quantum Electron.*, vol. QE-17, no. 1, pp. 15–22, Jan. 1981.

[11] D. Marcuse, C. R. Menyuk, and P. K. A. Wai, "Application of the Manakov-PMD equation to studies of signal propagation in optical fibers with randomly varying birefringence," *J. Lightw. Technol.*, vol. 15, no. 9, pp. 1735–1746, Sep. 1997.

[12] P. K. A. Wai and C. R. Menyuk, "Polarization mode dispersion, decorrelation, and diffusion in optical fibers with randomly varying birefringence," *J. Lightw. Technol.*, vol. 14, no. 2, pp. 148–157, Feb. 1996.

[13] J. M. Jacob and G. M. Carter, "Error-free transmission of dispersion-managed solitons at 10 Gbit/s over 24 500 km without frequency sliding," *Electron. Lett.*, vol. 33, no. 13, pp. 1128–1129, Jun. 1997.

[14] Q. Yu, S. Yan, S. Lee, Y. Xie, and A. E. Willner, "Loop-synchronous polarization scrambling for simulating polarization effects using recirculating fiber loops," *J. Lightw. Technol.*, vol. 21, no. 7, pp. 1593–1600, Jul. 2003.

[15] B. L. Heffner, "Automated measurement of polarization mode dispersion using Jones matrix eigenanalysis," *IEEE Photon. Technol. Lett.*, vol. 4, no. 9, pp. 1066–1069, Sep. 1992.

[16] B. Huttner, C. Geiser, and N. Gisin, "Polarization-induced distortions in optical fiber networks with polarization-mode dispersion and polarization-dependent loss," *IEEE J. Sel. Topics Quantum Electron.*, vol. 6, no. 2, pp. 317–329, Mar./Apr. 2000.

[17] H. Xu, H. Jiao, L. Yan, and G. M. Carter, "Measurement of distributions of differential group delay in a recirculating loop with and without loop-synchronous scrambling," *IEEE Photon. Technol. Lett.*, vol. 16, no. 7, pp. 1691–1693, Jul. 2004.

[18] H. Xu, B. S. Marks, L. Yan, C. R. Menyuk, and G. M. Carter, "A comparison of measurement techniques for differential group delay in a long-haul optical system," presented at the Optical Fiber Communication (OFC), Los Angeles, CA, Feb. 2004, Paper FI4.

[19] E. Corbel, "Concerns about emulation of polarization effects in a recirculating loop," presented at the Eur. Conf. Optical Communication (ECOC), Rimini, Italy, Sep. 2003, Paper Mo3.7.4.

[20] A. Galtarossa and L. Palmieri, "Reflectometric measurements of polarization properties in optical-fiber links," *IEEE Trans. Instrum. Meas.*, vol. 53, no. 1, pp. 86–94, Feb. 2004.

John Zweck received the B.Sc. degree (with honors) from the University of Adelaide, Adelaide, Australia, in 1988 and the Ph.D. degree in mathematics from Rice University, Houston, TX, in 1993.

He has performed research in differential geometry, human and computer vision, and optical communications. Since 2003, he has been an Assistant Professor in the Department of Mathematics and Statistics at the University of Maryland Baltimore County (UMBC), Baltimore. From 2000 to 2003, he was a Research Associate in the Department of Computer Science and Electrical Engineering at UMBC.

Li Yan (S'84–M'87) received the B.S. degree from the University of Science and Technology of China in 1982 and the M.S. and Ph.D. degrees from the University of Maryland, College Park, in 1986 and 1989, respectively, all in physics.

He joined the Faculty of Electrical Engineering at the University of Maryland Baltimore County, Baltimore, in 1990. His research areas include ultrafast and solid state lasers, optical communications, and nonlinear optics.

Dr. Yan is a member of the IEEE Lasers and Electro-Optics Society and the Optical Society of America.

Curtis R. Menyuk (SM'88–F'98) was born on March 26, 1954. He received the B.S. and M.S. degrees from the Massachusetts Institute of Technology (MIT), Cambridge, in 1976 and the Ph.D. degree from the University of California, Los Angeles (UCLA) in 1981.

He has worked as a Research Associate at the University of Maryland, College Park, and at Science Applications International Corporation, McLean, VA. In 1986, he became an Associate Professor in the Department of Electrical Engineering at the University of Maryland Baltimore County (UMBC), and he was the founding member of this department. In 1993, he was promoted to Professor. He was on partial leave from UMBC from Fall 1996 until Fall 2002. From 1996 to 2001, he worked part time for the Department of Defense, codirecting the Optical Networking Program at the DoD Laboratory for Telecommunications Sciences in Adelphi, MD, from 1999 to 2001. From 2001 to 2002, he was the Chief Scientist at PhotonEx Corporation. For the last 18 years, his primary research area has been on theoretical and computational studies of lasers, nonlinear optics, and fiber optic communications. He has authored or coauthored more than 190 archival journal publications as well as numerous other publications and presentations. He has also edited three books. The equations and algorithms that he and his research group at UMBC have developed to model optical fiber systems are used extensively in the telecommunications and photonics industry.

Dr. Menyuk is a member of the Society for Industrial and Applied Mathematics and the American Physical Society. He is a Fellow of the Optical Society of America. He is a former UMBC Presidential Research Professor.
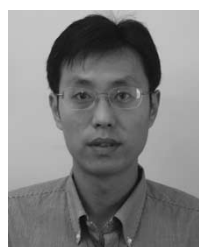
Hai Xu (M'05) received the B.E. degree in microwave engineering from the University of Electronics Science and Technology, Chengdu, China, in 1995, the M.S. degree in wireless engineering from the Beijing University of Posts and Telecommunications, Beijing, China, in 1998, and the Ph.D. degree in electrical engineering from University of Maryland Baltimore County (UMBC), Baltimore, in 2005.

Since then, he has been a Research Associate in the Department of Computer Science and Electrical Engineering at UMBC. He is also a Guest Researcher in the Information Technology Laboratory at the National Institute of Standards and Technology, Gaithersburg, MD. His research interests include optical fiber communication, polarization effects, and quantum key distribution.

Dr. Hai Xu is a member of the IEEE Lasers and Electro-Optics Society and the Optical Society of America.

Brian S. Marks (M'01), photograph and biography not available at the time of publication.

Gary M. Carter (M'82–SM'85) received the Ph.D. degree in atomic and molecular physics from the Massachusetts Institute of Technology (MIT), Cambridge.

He then went to MIT's Lincoln Laboratories, carrying out research in infrared nonlinear optics and infrared radar, then to GTE Laboratories carrying out research in nonlinear optics of polymers and semiconductors. Subsequently, he returned to MIT's Lincoln Laboratories, working in the areas of free space optical communications and nonlinear optical processes in semiconductor lasers. He joined the faculty at the University of Maryland Baltimore County (UMBC) in 1988 and, since then, has been carrying out research in biophotonics, semiconductor lasers, modelocking, and optical communications.

Prof. Carter is a Fellow of the Optical Society of America.